

Notes

Lamellar Alignment of Diblock Copolymers in an Electric Field

A. V. Kyrylyuk,* A. V. Zvelindovsky,*
G. J. A. Sevink, and J. G. E. M. Fraaije

Leiden Institute of Chemistry, Leiden University,
P.O. Box 9502, 2300 RA Leiden, The Netherlands

Received June 22, 2001

Revised Manuscript Received November 29, 2001

Applications in nanotechnology¹ have led to an increased interest toward the incorporation of externally applied field in current models for (micro)phase separation. In the past few years a large number of studies have addressed binary fluids,² solution,^{3–8} and melt^{9–17} behavior of block copolymers in an external electric field. Diblock copolymers form a variety of structures (lamellae, body-centered-cubic spheres, hexagonally packed cylinders, and gyroids), the morphology of which depends mainly on the temperature and the volume fraction of the polymer blocks.¹⁸ The reorientation of microdomains in the presence of an electric field has been observed experimentally for lamellar and cylindrical microstructures.^{9–11,17}

In previous theoretical works on this topic, Onuki and Fukuda^{15,16} have investigated the dynamics of undulation in two-dimensional lamellar systems both numerically and analytically. Amundson et al.^{9–11} have considered possible mechanisms of lamellar alignment by a theoretical analysis of electric-field-induced forces on different types of defects in microstructures. Besides these static calculations, they analyzed the influence of defect interactions on the defect mobility. Also, they calculated the velocity of a single wall defect for the special case of defect interactions on the basis of force balance on microdomains. We study a more general case of dynamics of mesophase formation in the framework of dynamic density functional theory (DDFT) for a diblock copolymer melt. Other groups are currently investigating the same application.¹⁹

Following the method of Amundson et al.,^{9–11} we assume that the different composition patterns within a diblock copolymer melt, and associated with them the space-dependent local permittivity produce different patterns in the electric field. Therefore, the electrostatic contribution to the free energy depends on the composition pattern. The free energy F due to the electrostatic interaction between the substance and the electric field is given by²⁰

$$F = F_0 - \frac{\epsilon_0}{2} \int_V \epsilon(\mathbf{r}) |\mathbf{E}(\mathbf{r})|^2 d\mathbf{r} \quad (1)$$

where F_0 is the free energy of the system in the absence of an applied field, $\epsilon(\mathbf{r})$ is the local dielectric constant of the material, ϵ_0 is the permittivity constant, $\mathbf{E}(\mathbf{r})$ is the electric field within the sample, and V is the volume of the sample.

The essential interaction which is taken into account is the long-range dipole–dipole interaction between polarized units. In this model, we do not consider the effects of chain deformation due to the anisotropy of the electric polarizability tensor of monomers, proposed by Gurovich.^{12–14} Onuki and Fukuda¹⁵ have shown that for most copolymers the ratio of strength of the Gurovich interaction and the induced dipolar interaction is much smaller than unity.

Expanding the dielectric constant to second order in the local composition, neglecting gradient terms, and solving the Maxwell equation, the anisotropic part of electrostatic contribution to the free energy can be written in Fourier space¹⁰

$$F - F_0 = \frac{1}{16\pi^3} \beta^{-1} \nu B \int \psi(\mathbf{k}) \psi(-\mathbf{k}) \left(\frac{\mathbf{k}}{k} \cdot \mathbf{e}_z \right)^2 d\mathbf{k} \quad (2)$$

where $k = |\mathbf{k}|$, $E_0 = |\mathbf{E}_0|$ is the strength of the uniformly applied field, \mathbf{e}_z is the unit vector in the direction z of the external electric field, $\beta^{-1} = k_B T$, and ν is the volume of the statistical unit (the same for all components). Here, the variable $\psi(\mathbf{k})$ is the Fourier transform of order parameter $\psi(\mathbf{r})$, which is equal to the deviation $\rho(\mathbf{r}) - \rho^0$ of the concentration $\rho(\mathbf{r})$ of one component of the diblock copolymer from the average value ρ^0 . The dimensionless parameter B incorporating the electric field strength is

$$B = \beta \epsilon_0 \nu \frac{2(\epsilon_A - \epsilon_B)^2}{(\epsilon_A + \epsilon_B)} E_0^2 \quad (3)$$

where ϵ_I is the dielectric constant of pure component I (A or B).

The free energy F_0 of a diblock copolymer melt in the absence of an external electric field is for a compressible melt consisting of ideal Gaussian chains in a mean-field environment. We do not truncate a free energy expansion (Cahn–Hilliard, Flory–Huggins–de Gennes, Oono–Puri) but retain the full polymer integral.^{21–25}

We consider a system of n diblock copolymer Gaussian chains of the length $N = N_A + N_B$. There are two concentration fields $\rho_I(\mathbf{r})$ of the beads of type I (A or B), two intrinsic chemical potentials $\mu_A(\mathbf{r})$ and $\mu_B(\mathbf{r})$, and two external potentials $U_A(\mathbf{r})$ and $U_B(\mathbf{r})$, conjugated to the concentrations fields ρ_A and ρ_B , respectively.

The intrinsic free energy functional $F_0[\rho]$ can be expressed as^{22–25}

$$F_0[\rho] = -\beta^{-1} \ln \frac{\Phi^n}{n!} - \sum_I \int_V U_I(\mathbf{r}) \rho_I(\mathbf{r}) d\mathbf{r} + \frac{1}{2} \sum_{I,J} \int_V \int_V \epsilon_{IJ}(|\mathbf{r} - \mathbf{r}'|) \rho_I(\mathbf{r}) \rho_J(\mathbf{r}') d\mathbf{r} d\mathbf{r}' + \frac{\kappa_H \nu^2}{2} \int_V (\sum_I \rho_I(\mathbf{r}) - \sum_I \rho_I^0)^2 d\mathbf{r} \quad (4)$$

where we have introduced the following conventional notations, Φ is the intramolecular partition function for the ideal Gaussian chain in the external field U_I , and $\epsilon_{IJ}(|\mathbf{r} - \mathbf{r}'|) = \epsilon_{JI}(|\mathbf{r} - \mathbf{r}'|)$ is a cohesive interaction parameter between beads of type I at \mathbf{r} and J at \mathbf{r}' .²¹ The Helfand's compressibility parameter is κ_H .^{22,23}

The intrinsic chemical potential μ_I , defined as the functional derivative of the free energy F , is a sum of two parts, $\mu_I^0(\mathbf{r})$ and $\mu_I^E(\mathbf{r})$. The expression for μ_I^0 can be found in our earlier papers.^{22–25} The chemical potential $\mu_I^E(\mathbf{r})$, containing the electric field contribution, has a simple form in Fourier space (see eq 2)

$$\mu_I^E(\mathbf{k}) = \beta^{-1} \nu B \left(\frac{\mathbf{k} \cdot \mathbf{e}_z}{k} \right)^2 (\rho_I(-\mathbf{k}) - (2\pi)^3 \rho_I^0 \delta(-\mathbf{k})) \quad (5)$$

where $\delta(-\mathbf{k})$ is a delta function.

To describe the diffusive dynamics of the concentration fields, we employ dynamic equations in a form similar to those for critical fluids (model B after Hohenberg and Halperin).²⁶ We are interested in a shallow quench, where the segregation is weak. The phase separation is then described by the modified time-dependent Ginzburg–Landau equation

$$\frac{\partial \rho_I(\mathbf{r})}{\partial t} = M \Delta \mu_I(\mathbf{r}) + \eta_I(\mathbf{r}, t) \quad (6)$$

where M is the mobility coefficient, which we assume to be a constant, and the same for all components; η_I is the random source.

Together, eqs 5 and 6 give the set of equations

$$\frac{\partial \rho_I(\mathbf{r})}{\partial t} = M \Delta \mu_I^0(\mathbf{r}) + M \beta^{-1} \nu B \frac{\partial^2 \rho_I(\mathbf{r})}{\partial z^2} + \eta_I(\mathbf{r}, t) \quad (7)$$

The equations of motion (7) were numerically integrated by means of a Crank–Nicolson scheme. As an example, we investigated the behavior of a model diblock copolymer melt A_8B_8 . The cubic grid is 64×64 in 2D and $32 \times 32 \times 32$ in 3D. As initial conditions, we consider a homogeneous distribution $\rho_I(\mathbf{r}) = \rho_I^0$. The dimensionless parameters are chosen as (for more details see refs 21 and 22): the dimensionless time step $\Delta \tau \equiv \beta^{-1} \nu M h^{-2} \Delta t = 0.5$ (h is the mesh size), the grid parameter $d \equiv a h^{-1} = 1.1543$ (a is the Gaussian chain bond length²¹), the noise scaling parameter $\Omega \equiv \nu^{-1} h^3 = 150$, exchange parameters $\chi_{IJ} \equiv (\beta/2\nu)[2\epsilon_{IJ}^0 - \epsilon_{JJ}^0 - \epsilon_{II}^0]$, and the dimensionless compressibility parameter $\kappa'_H \equiv \beta \kappa_H \nu = 30$.

From scaling analysis of the dynamical equations and the free energy, it follows that parameter controlling the electric field effect is BN , similar to the effective interaction strength χN (χ is the Flory–Huggins interaction parameter). All calculations with these scaled

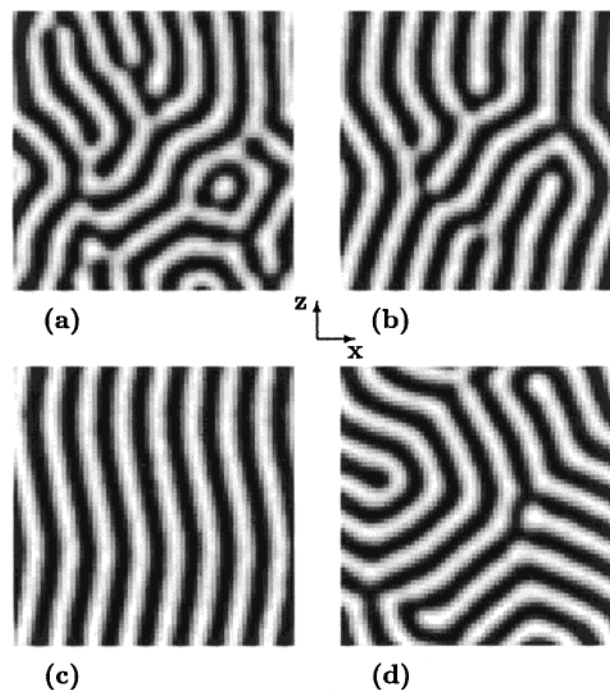


Figure 1. Morphologies of an A_8B_8 copolymer melt at dimensionless times (a) $\tau = 1000$, (b) $\tau = 6500$, and (c) $\tau = 30\,000$ in the presence of the external electric field and at (d) $\tau = 30\,000$ without electric field.

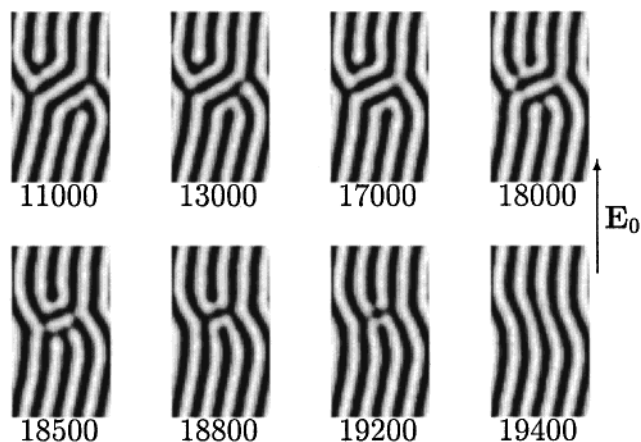


Figure 2. Slices of the density pattern of the same run as in Figure 1 at more frequent time intervals.

effective parameters yield the same result. For a typical experimental system, $N \sim 10^5$ monomers, $\beta \sim 10^{21} \text{ J}^{-1}$, $\nu \sim 10^{-28} \text{ m}^{-3}$ (molecular size), $E_0 \sim 10^6 \text{ V/m}$, $2(\epsilon_A - \epsilon_B)^2/(\epsilon_A + \epsilon_B) \sim 1$, and hence $BN \sim 0.1$. In the simulations we used $BN = 0.16$. Notice that the parameter BN scales quadratically with E_0^2 and linearly with N .

First we present simulation results in 2D shown in Figures 1 and 2. The interaction parameters are taken to be $\beta\epsilon_{AA}^0/\nu = \beta\epsilon_{BB}^0/\nu = 0.0$ and $\beta\epsilon_{AB}^0/\nu = 2.5$, so that $\chi N \approx 16.1$.

Figure 1a displays a stripe pattern obtained at an early stage ($\tau = 1000$) in the presence of an external electric field. The influence of the electric field is already present at this stage, but the effect is still small. In Figure 1b, which represents the result of an alignment process in an electric field at $\tau = 6500$, the lamellar structure is oriented rather well in direction of electric field but has some defects. These defects are distributed anisotropically, and they have preferable directions with

respect to the electric field. In Figure 1c,d, the difference in the behavior of the system, in the presence and in the absence of an electric field, is clearly visible. In the late stages ($\tau = 30\,000$) the picture with electric field (Figure 1c) completely differs from the phase separation pattern in the absence of electric field (Figure 1d), which consists of many local lamellar clusters without any global orientation. As can be seen from Figure 1c, the presence of an electric field results in a rather perfect lamellar structure. The lamellae are almost parallel to the direction of applied field.

A peculiar effect is the residual undulation: the final lamellae are not straight, as one might expect intuitively. The effect may be due to the freezing-in of the lamellar spacing in an earlier stage of the phase separation. Straight lamellae would be slightly thicker than the undulating lamellae, and therefore less lamellae would fit in the box. The transition of (thinner) undulating lamellae to (thicker) straight lamellae would have to involve symmetry breaking on the entire mesoscale, and this is apparently a kinetically very slow process. Rather, the patterns evolve through local defects.

The pictures of the alignment process can be explained in terms of nucleation and reorientation of ordered microdomains. First they grow up to a size that is sufficient. The second stage consists of reorientation of the microdomains, which is slow enough due to the small anisotropic component of the electrostatic contribution. The time scale of ordering of the diblock copolymer microstructure is much smaller than the time scale of the reorientation of the already ordered regions, as observed from Figure 1.

A more detailed picture of the defect movement is given in Figure 2. Two mechanisms of alignment are possible: alignment by selective disordering and alignment by defect movement.¹¹ Figure 2 illustrates the process of reorientation from the inclined to parallel lamellae by the recombination of the lamellar structure. Two types of structure changes are seen in Figure 2, namely joining and relinking of individual defects. We did not observe selective disordering in agreement with earlier predictions.¹¹

Results of simulations in 3D are shown in Figure 3. The diblock copolymer system now has interaction parameters $\beta\epsilon_{AA}^0/\nu = \beta\epsilon_{BB}^0/\nu = 0.0$ and $\beta\epsilon_{AB}^0/\nu = 3.0$ ($\chi N \approx 19.3$). The initial structure at $\tau = 500$ (Figure 3a) has a lot of defects. Under the influence of electric field the defects slowly disappear (Figure 3b). As a result, we observe an aligned lamellar microstructure with some defects (shown in Figure 3c), which completely differs from the observed lamellar pattern in the absence of electric field (and similar time stage) presented in Figure 3d. The 3D defect structure in Figure 3c is remarkably similar to the sketch in the original paper (Figure 2 in ref 11), based on experimental results for poly(styrene-*block*-methyl methacrylate) melt in an electric field.

The defect annihilation mechanism shown in Figure 2, where defects move toward each other and merge, is different from the defect annihilation mechanism we observed before in simulations of sheared block copolymer systems. In the sheared systems, defects are convected by the flow field.²⁵

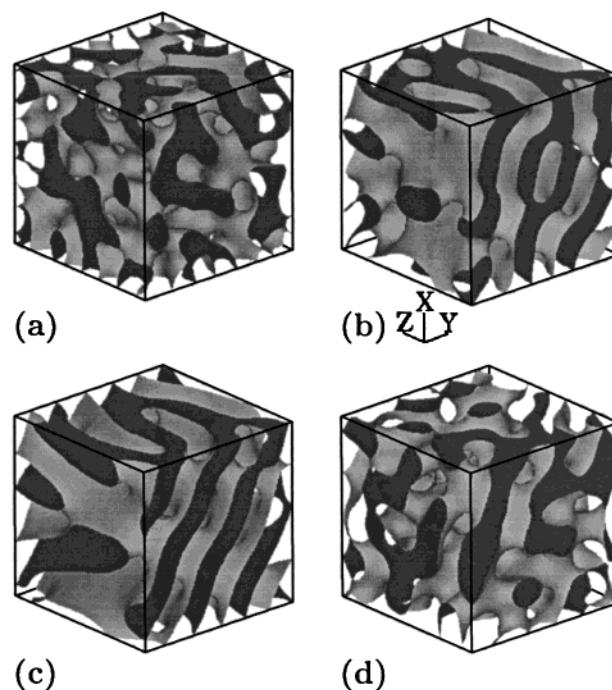


Figure 3. Isosurface representation of the A_8B_8 diblock copolymer melt for $\nu\rho_A = 0.5$ at (a) $\tau = 500$, (b) $\tau = 19\,000$, and (c) $\tau = 28\,000$ in the presence of the external electric field and at (d) $\tau = 28\,000$ without electric field.

In the Gurovich model,^{12–14} the electric field is coupled to the chain distribution function, and chains can be aligned individually. In the proposed model the coupling is through a mean field to the density rather than to the distribution function. Despite the drawback of the neglect of correlations, the model seems sufficient to capture the dominant effects. The process of alignment of block copolymer microstructure is dynamical by nature and, therefore, requires dynamical consideration for clarification the underlying mechanism.

Conclusion. We provide the first study of domain kinetics in time-dependent Ginzburg–Landau method in the mean-field approximation for the long-range dipole–dipole interaction in external electric fields. The free energy is calculated by the full path-integral method. Our model complements the static calculations^{9–11} by a detailed dynamic picture of lamellar alignment (Figure 2). Combination of full path-integral calculations and integration of the dynamic equations demonstrate that the domain alignment follows a relatively local defect movement, in each lamellae locally break up and merge again. The simulations of alignment dynamics and defect evolution can be used for tailoring of new experiments.

Acknowledgment. We gratefully acknowledge Karl Amundson for explaining the details of his work (refs 9–11). The authors thank Takashi Taniguchi and Takahiro Yukimura for stimulating discussions. NWO-DFG project DN 72-216 is gratefully acknowledged.

References and Notes

- (1) Park, M.; Harrison, C.; Chaikin, P. M.; Register, R. A.; Adamson, D. *Science* **1997**, *276*, 1401–1404.
- (2) Taniguchi, T.; Sato, K.; Doi, M. In *Statistical Physics*; Tokuyama, M., Stanley, H. E., Eds.; American Institute of Physics: Melville, NY, 2000; CP519, pp 581–583.

- (3) Wirtz, D.; Berend, K.; Fuller, G. G. *Macromolecules* **1992**, *25*, 7234–7246.
- (4) Wirtz, D.; Werner, D. E.; Fuller, G. G. *J. Chem. Phys.* **1994**, *101*, 1679–1686.
- (5) Wirtz, D.; Fuller, G. G. *Phys. Rev. Lett.* **1993**, *71*, 2236–2239.
- (6) Gurovich, E. *Macromolecules* **1995**, *28*, 6078–6083.
- (7) Böker, A.; Knoll, A.; Elbs, H.; Abetz, V.; Müller, A. H. E.; Krausch, G. *Macromolecules*, in press.
- (8) Böker, A.; Elbs, H.; Hänsel, H.; Knoll, A.; Zettl, H.; Urban, V.; Abetz, V.; Müller, A. H. E.; Krausch, G. Manuscript in preparation.
- (9) Amundson, K.; Helfand, E.; Davis, D. D.; Quan, X.; Patel, S. S.; Smith, S. D. *Macromolecules* **1991**, *24*, 6546–6548.
- (10) Amundson, K.; Helfand, E.; Quan, X.; Smith, S. D. *Macromolecules* **1993**, *26*, 2698–2703.
- (11) Amundson, K.; Helfand, E.; Quan, X.; Hudson, S. D.; Smith, S. D. *Macromolecules* **1994**, *27*, 6559–6570.
- (12) Gurovich, E. *Macromolecules* **1994**, *27*, 7063–7066.
- (13) Gurovich, E. *Phys. Rev. Lett.* **1995**, *74*, 482–485.
- (14) Gurovich, E. *Macromolecules* **1994**, *27*, 7339–7362.
- (15) Onuki, A.; Fukuda, J. *Macromolecules* **1995**, *28*, 8788–8795.
- (16) Fukuda, J.; Onuki, A. *J. Phys. II* **1995**, *5*, 1107–1113.
- (17) Morkved, T. L.; Lu, M.; Urbas, A. M.; Ehrichs, E. E.; Jaeger, H. M.; Mansky, P.; Russell, T. P. *Science* **1996**, *273*, 931–933.
- (18) Bates, F. S.; Fredrickson, G. H. *Phys. Today* **1999**, *52*, 32–38.
- (19) Taniguchi, T.; Yukimura, T. Private communication.
- (20) Landau, L. D.; Lifshitz, E. M. *Electrodynamics of Continuous Media*, 2nd ed.; Pergamon Press: New York, 1984; Vol. 8, pp 44–61.
- (21) Fraaije, J. G. E. M.; van Vlimmeren, B. A. C.; Maurits, N. M.; Postma, M.; Evers, O. A.; Hoffmann, C.; Altevogt, P.; Goldbeck-Wood, G. *J. Chem. Phys.* **1997**, *106*, 4260–4269.
- (22) Maurits, N. M.; van Vlimmeren, B. A. C.; Fraaije, J. G. E. M. *Phys. Rev. E* **1997**, *56*, 816–825.
- (23) van Vlimmeren, B. A. C.; Maurits, N. M.; Zvelindovsky, A. V.; Sevink, G. J. A.; Fraaije, J. G. E. M. *Macromolecules* **1999**, *32*, 646–656.
- (24) Maurits, N. M.; Sevink, G. J. A.; Zvelindovsky, A. V.; Fraaije, J. G. E. M. *Macromolecules* **1999**, *32*, 7674–7681.
- (25) Zvelindovsky, A. V.; Sevink, G. J. A.; van Vlimmeren, B. A. C.; Maurits, N. M.; Fraaije, J. G. E. M. *Phys. Rev. E* **1998**, *57*, R4879–R4882.
- (26) Hohenberg, P. C.; Halperin, B. I. *Rev. Mod. Phys.* **1977**, *49*, 435–479.

MA0110756